# Saturation transfer, continuous wave saturation, and saturation recovery electron spin resonance studies of chain-spin labeled phosphatidylcholines in the low temperature phases of dipalmitoyl phosphatidylcholine bilayers

## Effects of rotational dynamics and spin–spin interactions

Piotr Fajer, Anthony Watts, and Derek Marsh
Max-Planck-Institut für biophysikalische Chemie, Abteilung Spektroskopie, D-3400 Göttingen, Germany

ABSTRACT The saturation transfer electron spin resonance (STESR) spectra of 10 different positional isomers of phosphatidylcholine spin-labeled in the *sn*-2 chain have been investigated in the low temperature phases of dipalmitoyl phosphatidylcholine (DPPC) bilayers. The results of continuous wave saturation and of saturation recovery measurements on the conventional ESR spectra were used to define the saturation properties necessary for interpreting the STESR results in terms of the chain dynamics. Spin labels with the nitroxide group located in the center of the chain tended to segregate preferentially from the DPPC host lipids in the more ordered phases, causing spin–spin interactions which produced spectral broadening and had a very pronounced effect on the saturation characteristics of the labels. This was accompanied by a large decrease in the STESR spectral intensities and diagnostic line height ratios relative to those of spin labels that exhibited a higher degree of saturation at the same microwave power. The temperature dependence of the STESR spectra of the different spin label isomers revealed a sharp increase in the rate of rotation about the long axis of the lipid chains at ~25°C, correlating with the pretransition of gel phase DPPC bilayers, and a progessive increase in the segmental motion towards the terminal methyl end of the chains in all phases. Prolonged incubation at low temperatures led to an increase in the diagnostic STESR line height ratios in all regions of the spectrum, reflecting the decrease in chain mobility accompanying formation of the subgel phase. Continuous recording of the central diagnostic peak height of the STESR spectra while scanning the temperature revealed a discontinuity at ~14–17°C, corresponding to the DPPC subtransition which occurred only on the initial upward temperature scan, in addition to the discontinuity at 29–31°C corresponding to the pretransition which displayed hysteresis on the downward temperature scan.

## INTRODUCTION

The low temperature phases of lipid bilayers provide an interesting system for the study of the saturation transfer electron spin resonance (STESR)[1] spectra of phospholipids bearing a nitroxide spin label in the fatty acyl chain, for two main reasons. First, the low temperature phases constitute a system of high molecular packing density in which spin–spin interactions between nitroxides may occur and consequently influence the STESR spectra. Second, the sensitivity of STESR spectra to slow rotational diffusion (Thomas et al., 1976) offers the possibility to study the lipid chain motions in phases of different chain packing density and hence obtain information on the molecular dynamics in the different lipid gel phases.

Spin–spin interactions have already been shown to have a profound effect on STESR spectra in a recent study of spin-labeled $Ca^{2+}$-ATPase in sarcoplasmic reticulum membranes (Horváth et al., 1990). This marked influence on the STESR spectra arises from the greater intrinsic sensitivity of the effective spin-lattice relaxation time, $T_1$, than of the spin–spin relaxation time, $T_2$, to spin–spin interactions, because of the longer characteristic timescale of $T_1$ compared with $T_2$. Thus, STESR spectroscopy offers a sensitive method of investigating spin–spin interactions: essentially for the same reasons as those that give rise to the sensitivity to slow rotational diffusion.

The previous work on the $Ca^{2+}$-ATPase has suggested several mechanisms whereby spin–spin interactions may influence $T_1$ and hence provide dynamic information, e.g., translational diffusion rates, different from that obtained by the more classical STESR methods (Horváth et al., 1990). To be useful experimentally, this new aspect of STESR spectroscopy (i.e., to study spin ex-

Address correspondence to Dr. Marsh.

Dr. Fajer's present address is Institute of Biophysics, Department of Biological Science, Florida State University, Tallahassee, FL 32306-3015.

Dr. Watts' permanent address is Department of Biochemistry, University of Oxford, Oxford OX1 3QU, United Kingdom.

[1] *Abbreviations used in this paper:* ESR, electron spin resonance; STESR, saturation transfer ESR; $V_1$, first harmonic absorption spectrum recorded in phase with the magnetic field modulation; $V_2$, second harmonic absorption spectrum recorded in phase with the magnetic field modulation; $V_2'$, second harmonic absorption spectrum recorded 90°-out-of-phase with respect to the magnetic field modulation; CW, continuous wave; $P_{1/2}$, microwave power yielding half-saturation of the ESR line height in $V_1$ spectra; DPPC, 1,2-dipalmitoyl-*sn*-glycero-3-phosphocholine; DMPC, 1,2-dimyristoyl-*sn*-glycero-3-phosphocholine; *n*-SASL, *n*-(4,4-dimethyl-oxazolidine-*N*-oxyl)stearic acid; *n*-PCSL, 1-acyl-2-[*n*-(4,4-dimethyl-oxazolidine-*N*-oxyl)stearoyl]-*sn*-glycero-3-phosphocholine.


0006-3495/92/04/879/13 $2.00

change and dipolar interactions) requires a more detailed understanding of the influence of spin–spin interactions on the saturation behavior of spin labels and the manifestation of these interactions in STESR spectra. Progress in this direction is made here by a study of the consequences of spin label clustering in phospholipid gel phases.

The motions of spin labeled lipid chains in gel phase bilayers have previously been shown to lie in the range of optimal sensitivity of STESR spectroscopy (Marsh, 1980). These latter studies were confined to a spin label situated close to the polar headgroup end of the chain and provided information on the overall rotation about the lipid chain axis. To obtain information relating to segmental motion of the chains, it is necessary to explore other positions of chain labeling. This is done here for 10 different positional isomers of spin-labeled phosphatidylcholine in bilayers of dipalmitoylphosphatidylcholine. Continuous wave saturation studies are also performed so as to allow for the varying saturation characteristics in comparing the dynamic properties of the different positional isomers.

The previous studies concentrated only on the behavior in the $L_{\beta'}$, gel phase and in the $P_{\beta'}$, intermediate or ripple phase of DPPC bilayers. It is known that the $L_{\beta'}$, phase is metastable at low temperatures and on prolonged incubation converts to the stable subgel phase ($L_c$) which then can undergo a thermotropic transition to the stable $L_{\beta'}$, phase at the subtransition which lies lower in temperature than the pretransition (Chen et al., 1980; Füldner, 1981). For this reason studies are also made on the effects of low temperature incubation on the saturation transfer spectra of the chain-labeled lipids in the gel phase. A continuous temperature scanning version of STESR spectroscopy was also developed to study the subtransition of incubated DPPC samples.

## MATERIALS AND METHODS

### Materials

DPPC was obtained from Fluka (Buchs, Switzerland). Positional isomers of spin labeled stearic acid, *n*-SASL, were synthesized as described by Marsh and Watts (1982) and acylated to egg lysophosphatidylcholine, yielding the *n*-PCSL spin-labeled phosphatidylcholines as detailed in the same reference. DPPC and *n*-PCSL spin label (0.1 or 1.0 mol%) were codissolved in chloroform which was then evaporated with a nitrogen gas stream, and the sample was finally dried under a vacuum for at least 3 h. The dry lipid was dispersed in 0.1 M KCl, 10 mM Tris, pH 8.0 at a concentration of 100 mg/ml and hydrated by heating above the gel-fluid phase transition temperature (41°C) with vortex mixing for ~5 min. Aliquots (100 μl) of the dispersion were introduced into 1-mm diameter glass capillaries and centrifuged at full speed in a bench top centrifuge for ~10 min. Excess supernatant was removed and, where necessary, the samples were homogenized and trimmed to 5-mm length. Experiments were also performed with line samples which filled the full active region of the microwave cavity. The effects of microwave and modulation field inhomogeneities on the STESR spectra have been characterized previously (Fajer and Marsh, 1982; Hemminga et al., 1984).

### ESR Spectroscopy

ESR spectra were recorded on a Varian Century Line 9 GHz spectrometer (Varian Associates, Palo Alto, CA), with the Varian E-321, rectangular $TE_{102}$ cavity and double-wall quartz dewar. Samples were centered within a standard 4-mm quartz tube, using a specially designed concentric sample holder. The samples were equilibrated with air; the saturation properties of chain-labeled lipids in gel phase bilayers are not very sensitive to the presence of oxygen (Marsh, 1982; Kusumi et al., 1982). For 5-PCSL in DPPC at 1°C, the half-saturation power was measured to be 41 mW in aerated buffer and 37 mW when degassed. Cavity Q and $H_1$ microwave field were determined as described in Fajer and Marsh (1982). Saturation transfer ESR spectra were recorded in the second harmonic, 90° out-of-phase, absorption ($V_2'$) mode at a modulation frequency of 50 kHz, a modulation amplitude of 5 G and a mean microwave field at the sample of $\langle H_1^2 \rangle = 0.25^2$ G$^2$. Quadrature-phase ($V_2'$) nulls at subsaturating power were <1% of the in-phase ($V_2$) signal amplitude in all cases. Continuous temperature scans were performed by locking the spectrometer to the C′ negative peak in the central region of the $V_2'$-mode STESR spectrum (see Thomas et al., 1976 for definition of STESR line heights). This was done by feeding the double-modulated second harmonic 90° out-of-phase output signal from the low frequency (1 kHz) detection channel to the field control circuit of the field-frequency lock unit (cf Marsh and Watts, 1981). Critical coupling was maintained by servo-adjustment of the coupling iris with continuous monitoring of the microwave detector current. Output of the C′ STESR line height was displayed against the linearized thermocouple output on an *x-y* recorder. CW saturation experiments were carried out in the in-phase, first harmonic absorption ($V_1$) mode, by recording the line height at the turning point of the low-field hyperfine manifold. The microwave power corresponding to half-saturation, $P_{1/2}$, was obtained by extrapolation of the linear dependence on $\sqrt{P}$ at low power. Rotational correlation time calibrations of the diagnostic STESR line height ratios (Thomas et al., 1976), in terms of the isotropic rotation of spin-labeled hemoglobin, are given in Fajer and Marsh (1982). Saturation recovery experiments were performed at 9 GHz on an instrument described by Huisjen and Hyde (1974), and data were collected and analyzed as described in Fajer et al. (1986).

## RESULTS

### Continuous wave saturation

STESR studies on the chain dynamics of the spin-labeled lipids first requires characterization of the ESR saturation properties of the different *n*-PCSL positional isomers. In CW saturation experiments, the signal intensity, $S$, increases with the microwave field strength, $H_1$, according to the factor $H_1/(1 + \gamma^2 H_1^2 T_1^{eff} T_2^{eff})^p$, assuming Lorentzian spin packet line shapes (see Appendix):

$$S = S_o \cdot H_1/(1 + \gamma^2 H_1^2 T_1^{eff} T_2^{eff})^p \qquad (1)$$

where $S_o$ is independent of $H_1$ and the denominator on the right-hand side of the equation represents the effects of saturation, with $p = \frac{1}{2}$ for inhomogeneously broad-

ened lines and $p = 1$ for homogeneously broadened absorption line shapes (as for the low-field line in first derivative powder spectra).[2] For lipid spectra in the gel phase the saturation behavior approximates to the inhomogeneous case (Marsh, 1982). The values of the microwave power for half-saturation, $P_{1/2}$, deduced from CW saturation measurements on the different *n*-PCSL spin-label positional isomers in the gel phase of DPPC at 1°C are given in Fig. 1. The corresponding values of the mean-square microwave magnetic field at half-saturation are defined by the condition: $S/(S_0H_1) = \frac{1}{2}$ in Eq. 1, and are given by:

$$\langle H^2_{1,1/2}\rangle = C_{1/2}/\gamma^2 T_1^{\text{eff}} T_2^{\text{eff}}, \qquad (2)$$

where $T_1^{\text{eff}}$, $T_2^{\text{eff}}$ are the effective longitudinal and transverse relaxation times of the spin label and $\gamma$ is the gyromagnetic ratio of the electron. The constant $C_{1/2}$ in Eq. 2 has the value 1 for homogeneous broadening (Lorentzian absorption line shape, corresponding to $p = 1$ in Eq. 1) and 3 for inhomogeneous broadening (corresponding to $p = \frac{1}{2}$ in Eq. 1). The values of $P_{1/2}$ in Fig. 1 are seen to reach a maximum, corresponding to a minimum in the $T_1^{\text{eff}}\,T_2^{\text{eff}}$ product, towards the center of the chain ($n$ = 8–10). This variation in the saturation behavior can be attributed to spin–spin interactions arising from a partial segregation of the $n$ = 8–10 spin label positional isomers in the DPPC gel phase. This is indicated further by comparison with the B/S ratio, which is a measure of the spin–spin broadening in the conventional ESR spectra (see Fig. 4, later) and has a similar dependence upon the nitroxide position, $n$, to that of $P_{1/2}$ (Fig. 1).

A quantity that is also related to the CW saturation properties is the ratio, $V'_2/V_2$, of the out-of-phase to the in-phase signal heights in the second harmonic absorption ESR spectra (cf Thomas et al., 1976). This quantity is defined as the ratio of the maximum peak height in the $V'_2$-display to the maximum peak-to-peak height in the $V_2$-display, and its values as a function of spin-label position are also given in Fig. 1. A sharp decrease is observed in the upper part of the chain, corresponding to the increases found on approaching the maxima of the other two parameters in the central region of the chain. The subsequent increase towards the end of the chain is not so pronounced however, because the $V'_2/V_2$ parameter is sensitive not only to the relaxation times but also to the molecular dynamics (cf Horváth and Marsh, 1983) which increase towards the methyl end of the chain. The values of $V'_2/V_2$ are therefore not so large at the methyl end of the chain as they are at the polar headgroup end of the chain.

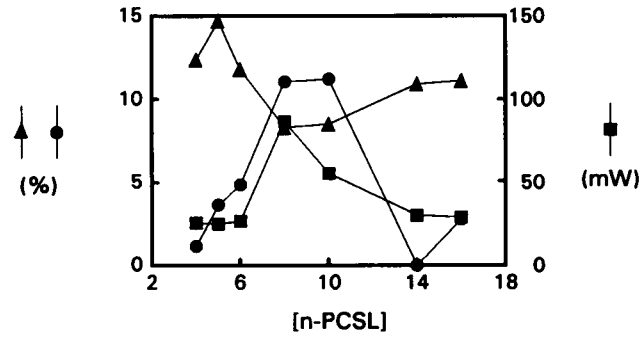


FIGURE 1 Positional dependence, $n$, of the CW saturation properties of n-PCSL phosphatidylcholine spin label positional isomers (0.1 mol%) in gel phase DPPC bilayers at 1°C. (■) half-saturation power, $P_{1/2}$ (mW), for the $V_1$-mode spectra; (▲) out-of-phase/in-phase ratio, $V'_2/V_2$ (%), in the second harmonic spectra; (●) spin–spin broadening ratio, B/S (%), in the $V_1$-mode spectra (see caption to Fig. 4, below for definition). Qualitatively similar results were obtained for a line sample with 1 mol% spin label concentration.

The correlation between the second harmonic out-of-phase/in-phase signal height ratio, $V'_2/V_2$, and the mean square microwave magnetic field at half saturation, $\langle H^2_{1,1/2}\rangle$, is given in Fig. 2 for different *n*-PCSL positional isomers at different temperatures. The linear proportionality with the $T_1^{\text{eff}}T_2^{\text{eff}}$ product (cf Eq. 2) that is evident in the figure divides the data into two groups: one group comprising the spin labels ($n$ = 8, 10) that show spin–

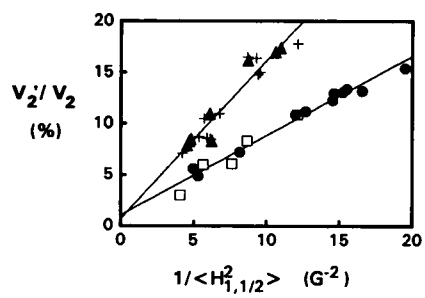


FIGURE 2 Dependence of the out-of-phase/in-phase ratio, $V'_2/V_2$ (%), on the inverse microwave field intensity at half-saturation, $1/\langle H^2_{1,1/2}\rangle$, for the second harmonic absorption ESR spectra of *n*-PCSL phosphatidylcholine spin labels (0.1 mol%) at different temperatures in the gel phase of DPPC bilayers. (●) 4-PCSL; (▲) 8-PCSL; (+) 10-PCSL; (□) 14-PCSL. Full lines are linear regressions.

[2]If the inhomogeneous broadening is so large that saturation broadening has no effect on the powder line shape, the line height will saturate in the same way as does the integrated intensity of the individual component Lorentzian lines, i.e., $p = 1/2$. In the absence of inhomogeneous broadening, the first-derivative powder spectrum has the homogeneous absorption line shape at the $\theta = 0$ turning points (Weil and Hecht, 1963; Hubbell and McConnell, 1971) and therefore the line heights of the outer hyperfine peaks will saturate as does that of a Lorentzian absorption line, i.e., $p = 1$.

spin interactions, and the other group comprising the labels that are located closer to the two ends of the chain ($n = 4, 14$) and display the smaller gradient in Fig. 2. These results can be understood, if it is assumed (as found in spectral simulations) that the out-of-phase/in-phase ratio is proportional to the product $\omega_m T_1^{eff}$, where $\omega_m$ is the modulation frequency (Thomas & McConnell, 1974; Thomas et al., 1976), and is not strongly dependent on $T_2^{eff}$. The gradients of the dependence on $1/\langle H_{1,1/2}^2 \rangle$ in Fig. 2 would then be inversely proportional to $T_2^{eff}$, which accounts for the larger gradient obtained with the labels in the center of the chain that exhibit spin–spin broadening (cf Fig. 1). Quantitatively, the ratio of the gradients in Fig. 2 is 2.0, whereas the inverse ratio of the aggregate effective $T_2$ values given in Table 1 is 2.1.

TABLE 1 **Effective longitudinal ($T_1$) and transverse ($T_2$) relaxation times of *n*-PCSL phosphatidylcholine spin label positional isomers (0.1 mol %) in gel phase DPPC bilayers at 1°C**

| $n$ | $\langle H_{1,1/2}^2 \rangle$ ($G^2$) | $T_1$ (s) | $T_2^{eff}$ (s) | |
|---|---|---|---|---|
| 4 | 0.055 | $9.2 \times 10^{-6}$ | $6.4 \times 10^{-9}$* | $1.9 \times 10^{-8}$‡ |
| 6 | 0.075 | $8.4 \times 10^{-6}$ | $5.1 \times 10^{-9}$* | $1.5 \times 10^{-8}$‡ |
| 8 | 0.22 | $7.7 \times 10^{-6}$ | $1.9 \times 10^{-9}$* | $5.7 \times 10^{-9}$‡ |
| 10 | 0.2 | $5.7 \times 10^{-6}$ | $2.8 \times 10^{-9}$* | $8.5 \times 10^{-9}$‡ |
| 14 | 0.11 | $5.3 \times 10^{-6}$ | $5.8 \times 10^{-9}$* | $1.7 \times 10^{-8}$‡ |
| 16 | 0.08 | $1.3 \times 10^{-5}$ | $3.0 \times 10^{-9}$* | $8.9 \times 10^{-9}$‡ |

Determined from saturation recovery ($T_1$) and CW saturation (mean square half-saturation microwave field, $\langle H_{1,1/2}^2 \rangle$) experiments.
*Calculated from Eq. 2, assuming homogeneous broadening.
‡Calculated from Eq. 2, assuming inhomogeneous broadening.

## Saturation recovery

Saturation recovery experiments were performed by recording the central ($M_I = 0$) hyperfine line of the 4-, 6-, 8-, 10-, 14-, and 16-PCSL labels in DPPC bilayers at 1°C. The recovery curves were fitted adequately with a single exponential recovery yielding the effective values of $T_1$ presented in Table 1. Multi-exponential fits were not justified by the data. As for the $V'_2/V_2$ and CW saturation results in Fig. 1, faster relaxation is found for the labels in the middle of the chain (8- and 10-PCSL), than for those close to the ends of the chain (4- and 16-PCSL). The value of the effective $T_1$ for 14-PCSL is surprisingly low. Effective values for $T_2$ deduced from the CW saturation and saturation recovery results, according to Eq. 2, are also given in Table 1. The values deduced assuming homogeneous broadening are smaller than the expected intrinsic $T_2$ values, presumably because of the effects of inhomogeneous broadening on the saturation behavior. The relatively large differences in the effective values of $T_2$ between the different spin label isomers may be due in part also to uncertainties in the degree of inhomogeneous broadening. Alternatively there may be a heterogeneity in the degree of clustering of the 8- and 10-PCSL positional isomers, giving a fast relaxing component that is not detected in the saturation recovery experiments, but is reflected in the CW saturation experiments. The differences observed in the $T_1$ relaxation rate due to spin–spin interactions are too small to have an appreciable direct influence on the effective $T_2$ values. However, due to the difficulty in performing multi-exponential fits, it is likely that the intrinsic effects of spin–spin interactions will be greater than those recorded by the effective $T_1$ values given in Table 1 (cf Yin et al., 1987).

Heisenberg exchange is a cross-relaxation process which gives rise to an alleviation of saturation by spin transfer within the powder line shape (e.g., Eastman et al., 1969). Assuming that the additional contribution, $(1/T_1^{eff})_{ex}$, of spin–spin interactions to the effective $T_1$ relaxation rate of 10-PCSL relative to 4- and 16-PCSL is dominated by diffusion-controlled Heisenberg exchange (cf Molin et al., 1980; Sachse et al., 1987) then:

$$(1/T_1^{eff})_{ex} = (1/3)k_{coll}c, \quad (3)$$

where $c = 10^{-3}$ is the mole fraction of spin label, and the enhanced bimolecular collision rate constant would be estimated to be: $k_{coll} = 2 - 3 \times 10^8\ s^{-1}$ (see also[3]). This is comparable with the collision rates measured in fluid lipid bilayers (Sachse et al., 1987). Because the translational diffusion rates in gel phase bilayers are ~2–3 orders of magnitude slower than in the fluid phase (Clegg and Vaz, 1985), this suggests that the local concentration of the *n*-PCSL isomers with the spin label located in the middle of the chain is increased by ~100–1,000 fold in the gel phase. Exchange at this rate is unlikely to affect the values of $T_2^{eff}$ as markedly as those of $T_1^{eff}$, however. The additional linebroadening seen in the conventional spectra for these positional isomers may be due partly also to static dipolar broadening.

A further confirmation of the influence of spin–spin interactions on the effective $T_1$ relaxation comes from the dependence of the second harmonic out-of-phase/in-phase signal height ratio on concentration of the 5-PCSL label that is given in Fig. 3. This label does not have the strong tendency to segregation found for the labels positioned in the center of the chain. Assuming as above that the $V'_2/V_2$ ratio is proportional to the effective $T_1$, the concentration dependence seen in Fig. 3 conforms to that expected from the more general form of Eq. 3

[3]Similar values are obtained by using the more general version of Eq. 3, together with a redistribution factor $Z = 0.12$ (cf following paragraph).

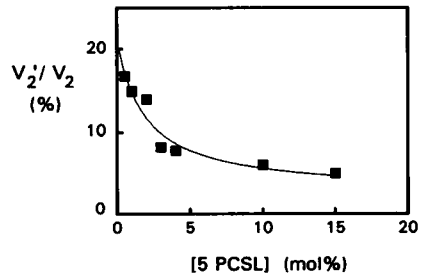


FIGURE 3 Spin label concentration dependence of the out-of-phase/in-phase signal height ratio, $V_2'/V_2$, for the second harmonic absorption ESR spectra of the 5-PCSL phosphatidylcholine spin label at 1°C in the gel phase of DPPC bilayers. Full line is an optimized fit (simplex) to Eq. 4, obtained with the parameters: $k_{coll}T_1^\circ = 100$, $Z = 0.12$, and $(V_2'/V_2)_o = 21\%$.

(Eastman et al., 1969; Marsh and Horváth, 1992):

$$(V_2'/V_2) = (V_2'/V_2)_o \cdot \left[1 + \frac{1}{2} Z \cdot k_{coll} \cdot T_1^\circ \cdot c\right] \Big/ \left[1 + \frac{1}{2} k_{coll} \cdot T_1^\circ \cdot c\right], \quad (4)$$

where $(V_2'/V_2)_o$ and $T_1^\circ$ are the values of $V_2'/V_2$ and $T_1$, respectively, in the absence of exchange, and $1/Z$ is the redistribution factor of the spin packets on exchange. From the optimized fit to the data in Fig. 3, and taking a value of $T_1^\circ = 9$ μs from Table 1, the collision rate constant is estimated to be $k_{coll} = 1.1 \times 10^7\ s^{-1}$. This value is 40 times slower than that in fluid bilayers and therefore is more appropriate to the gel phase (Clegg and Vaz, 1985). The value of $Z = 0.12$ obtained from the fit corresponds to a larger degree of redistribution on exchange than the factor of $Z = \frac{1}{3}$ expected for simple redistribution between the three hyperfine manifolds. This additional degree of freedom arises from the angular distribution of spin packets for a single manifold within the powder line shape, subject to restrictions arising from the orientation of the 5-PCSL label in the gel phase (Marsh and Horváth, 1992). Nuclear relaxation is not anticipated to play an overwhelming role because, for long rotational correlation times, the electron nuclear dipolar relaxation mechanism is likely to be relatively ineffective (cf Popp and Hyde, 1982). Although, if nuclear relaxation does have any influence, it will tend to increase the effective value of $Z$ for the $m_I = 0$ manifold.

## Saturation transfer ESR

Typical second harmonic STESR spectra and conventional ESR spectra of the different $n$-PCSL phosphatidylcholine spin label positional isomers in gel phase DPPC bilayers are given in Fig. 4. The conventional ESR spectra (with the exception of 16-PCSL) are all close to the rigid limit of sensitivity to rotational motion on the conventional nitroxide ESR timescale. The conventional ESR spectra do differ, however, between the different $n$-PCSL spin labels in that spin–spin broadening is evident for those positional isomers located close to the center of the chain ($n$ = 6–12). This is seen from the fact that the spectrum does not return to the baseline at the extremes of the 100 G scan, but is offset by a relative amount B/S, where $S$ is the maximum peak-to-peak height (see caption to Fig. 4 for definition).

The STESR spectra indicate a high degree of motional restriction for the labels closer to the polar headgroup (4-PCSL and 6-PCSL) in gel phase DPPC bilayers. An increased mobility is evident close to the terminal methyl end of the chain (14-PCSL and 16-PCSL). For 16-PCSL this even extends to incipient motional narrowing in the conventional spectrum. The STESR spectra from the positional isomers close to the center of the chain (8-PCSL and 12-PCSL) have considerably reduced relative intensity in the diagnostic regions $L''$, $C'$ and $H''$, which for equivalent degrees of saturation would be characteristic of an apparently faster motion. This reduction in intensity correlates with the spin–spin broadening observed in the conventional ESR spectra and arises at least in part, from the faster effective $T_1$ relaxation that is evident from the decreased degree of saturation for these samples in the CW saturation and saturation recovery experiments discussed above. Such effects are in agreement with simulations of the influence of decreased $T_1$ on $V_2'$ spin label STESR spectra (Thomas et al., 1976). In addition, contributions are also likely from a change in the lipid chain dynamics resulting from the spin label clustering.

The dependence of the diagnostic STESR line height ratios in the low-field, central and high-field manifolds of the spectrum (see Thomas et al., 1986, for definition) on the position of the spin label in the chain are given in Fig. 5. The most obvious feature of these positional profiles is the deep trough in the $C'/C$ ratio for the spin labels located in the center of the chain that arises from spin–spin interactions and other effects consequent on the partial segregation of these particular positional isomers in the DPPC gel phase. Superimposed on this trough, a gradual decrease in line height ratio (which is also seen for the $L''/L$ ratio) occurs on going from the upper part of the chain towards the terminal methyl ends, corresponding to increasing rates of chain segmental motion. Rather similar results to those of Fig. 5 were obtained for the line samples with spin label concentration of 1 mol%, except that a central trough was also observed for the $L''/L$ and $H''/H$ ratios (cf Fig. 4). This latter observation, together with the preferential sensitivity of the $C'/C$ ratio, suggests that the distortions of the

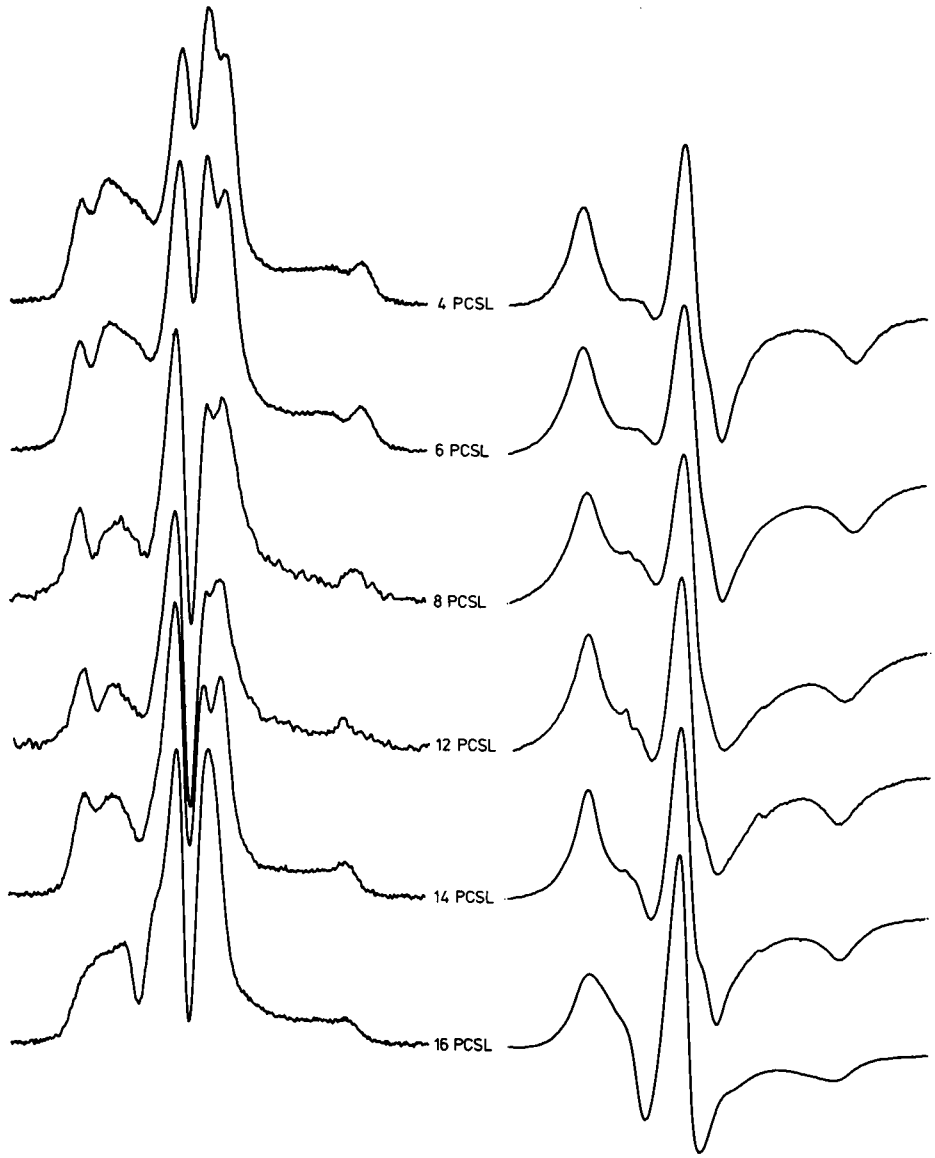


FIGURE 4 Second harmonic out-of-phase STESR spectra ($V'_2$ display, *left-hand panel*) and first harmonic in-phase conventional ESR spectra ($V_1$ display, *right-hand panel*) of *n*-PCSL phosphatidylcholine spin label positional isomers (1 mol%) in gel phase DPPC bilayers recorded at 1°C after overnight incubation at 0°C. The parameter B/S, which is defined as the ratio of the difference between the signal heights at the extremes of the scan (i.e., the sum of the absolute values of the departures from the baseline) to the peak-to-peak height of the central hyperfine line, indicates the degree of spin–spin broadening in the conventional spectra. Total scan width = 100 *G*.

line height ratio profile are determined at least in part by the spin–spin broadening that is apparent in the conventional spectra.

The dependence of the diagnostic STESR line height ratios on spin label concentration for 5-PCSL in gel phase DPPC is given in Table 2. This label does not exhibit the pronounced tendency to phase separation evident for the labels located in the center of the chain. The STESR line height ratios decrease progressively with increasing spin label concentration, but at 15 mol% the degree of reduction is not as great as the depth of the trough in the *n*-dependence seen in Fig. 5. Either the clustering of the 8- and 10-PCSL labels gives rise to a higher local concentration than 15 mol% or, as is likely, the lipid chain mobility in the clustered regions is greater than that in the DPPC gel phase.

In general, the STESR spectra were recorded after incubation of the samples at low temperature in the gel

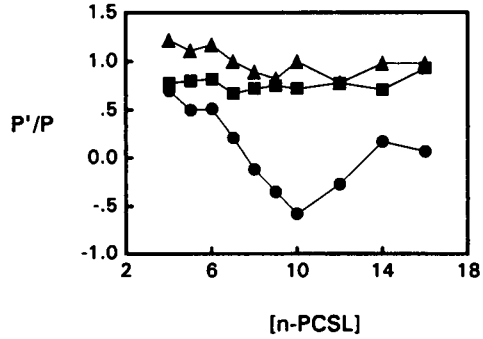


FIGURE 5 Positional dependence, $n$, of the diagnostic line height ratios in the second harmonic out-of-phase STESR spectra ($V'_2$ display) of $n$-PCSL phosphatidylcholine spin label positional isomers (0.1 mol%) in gel phase DPPC bilayers recorded at 1°C after overnight incubation at 0°C. (▲) low-field line height ratio, $L''/L$; (●) central line height ratio, $C'/C$; (■) high-field line height ratio, $H''/H$.

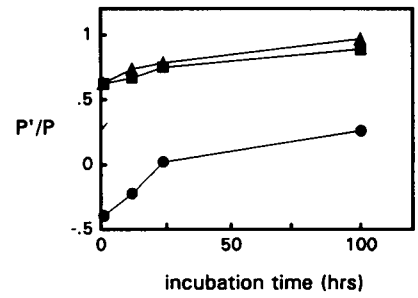


FIGURE 6 Time dependence of the relaxation in the diagnostic line height ratios for the STESR spectra ($V'_2$ display) of 6-PCSL spin-labeled phosphatidylcholine in gel phase DPPC dispersions, on incubation at 1°C after heating to 50°C. (▲) low-field line height ratio, $L''/L$; (●) central line height ratio, $C'/C$; (■) high-field line height ratio, $H''/H$.

phase. This incubation gave rise to relaxation of the gel phase to a more rigid state, as indicated by the change in the STESR diagnostic line height ratios of the 6-PCSL spin label with time of incubation at 1°C that is shown in Fig. 6. A considerable increase in all the diagnostic line height ratios, particularly $C'/C$, that corresponds to a decrease in chain mobility is observed after prolonged incubation. The half-time for the relaxation is approximately 18–32 h, with the faster rate being registered by the $C'/C$ ratio that is preferentially sensitive to long axis rotation (Marsh, 1980). For the spin label positional isomers located at the center of the chain, prolonged incubation at low temperature gave rise to an increase in spin–spin broadening of the conventional ESR spectra (cf Fig. 4), indicating a further tendency to phase separation of the label from the DPPC host lipid. The saturation transfer ESR spectra nonetheless exhibited a marked increase in the diagnostic line height ratios also for these positional isomers, and the half-saturation power was not appreciably affected, whereas the STESR out-of-phase/in-phase ratio decreased.

TABLE 2 **Spin label concentration dependence of the low-field ($L''/L$), central ($C'/C$) and high-field ($H''/H$) diagnostic line height ratios in the $V'_2$ STESR spectrum of the 5-PCSL phosphatidylcholine spin label at 1°C in the gel phase of DPPC bilayers**

| Concentration (mol %) | $L''/L$ | $C'/C$ | $H''/H$ |
|---|---|---|---|
| 0.5 | 1.09 | 0.52 | 0.85 |
| 1.0 | 1.08 | 0.51 | 0.84 |
| 2.0 | 1.06 | 0.50 | 0.83 |
| 3.0 | 1.07 | 0.50 | 0.83 |
| 4.0 | 1.00 | 0.41 | 0.69 |
| 5.0 | 1.01 | 0.42 | 0.73 |
| 10.0 | 0.94 | 0.29 | 0.73 |
| 15.0 | 0.85 | 0.04 | 0.69 |

The temperature dependence of the diagnostic line height ratios of the different $n$-PCSL spin label positional isomers in DPPC bilayers is given in Fig. 7. In spite of the difference in the absolute values of the STESR line height ratios for the different isomers, most revealed a similar response to the pretransition and main transition of the DPPC bilayers. As observed previously for 5-PCSL (Marsh, 1980), the greatest change at the pretransition occurs for the central, $C'/C$, line height ratio. It should also be mentioned that a similar temperature dependence was observed for 5-PCSL in a DPPC sample that had been extensively degassed (data not shown), indicating a lack of effect of oxygen in this region of the gel phase. In general, the change observed in the $L''/L$ and $H''/H$ ratios at the pretransition was smaller for the labels at the two ends of the chain (especially for 4-PCSL) than for the labels in the center of the chain (see Fig. 7). This difference is, at least partly, coupled with the difference in the temperature dependence of the saturation properties for the different positional isomers. The values of $\langle H^2_{1,1/2} \rangle$ decrease with increasing temperature for labels located at the center of the chain, whereas they increase for the labels closer to the chain ends (data not shown). The most likely reason for this lies in the dissolution of the spin label clusters at higher temperature, hence, alleviating the effects of spin–spin interaction.

The downward temperature scans subsequent to the initial upward scans in Fig. 7 reveal a mestastability or hysteresis correlating with that indicated by the time-dependent relaxation effects given in Fig. 6. For this reason, the temperature dependence was studied with higher resolution on incubated samples by continuously

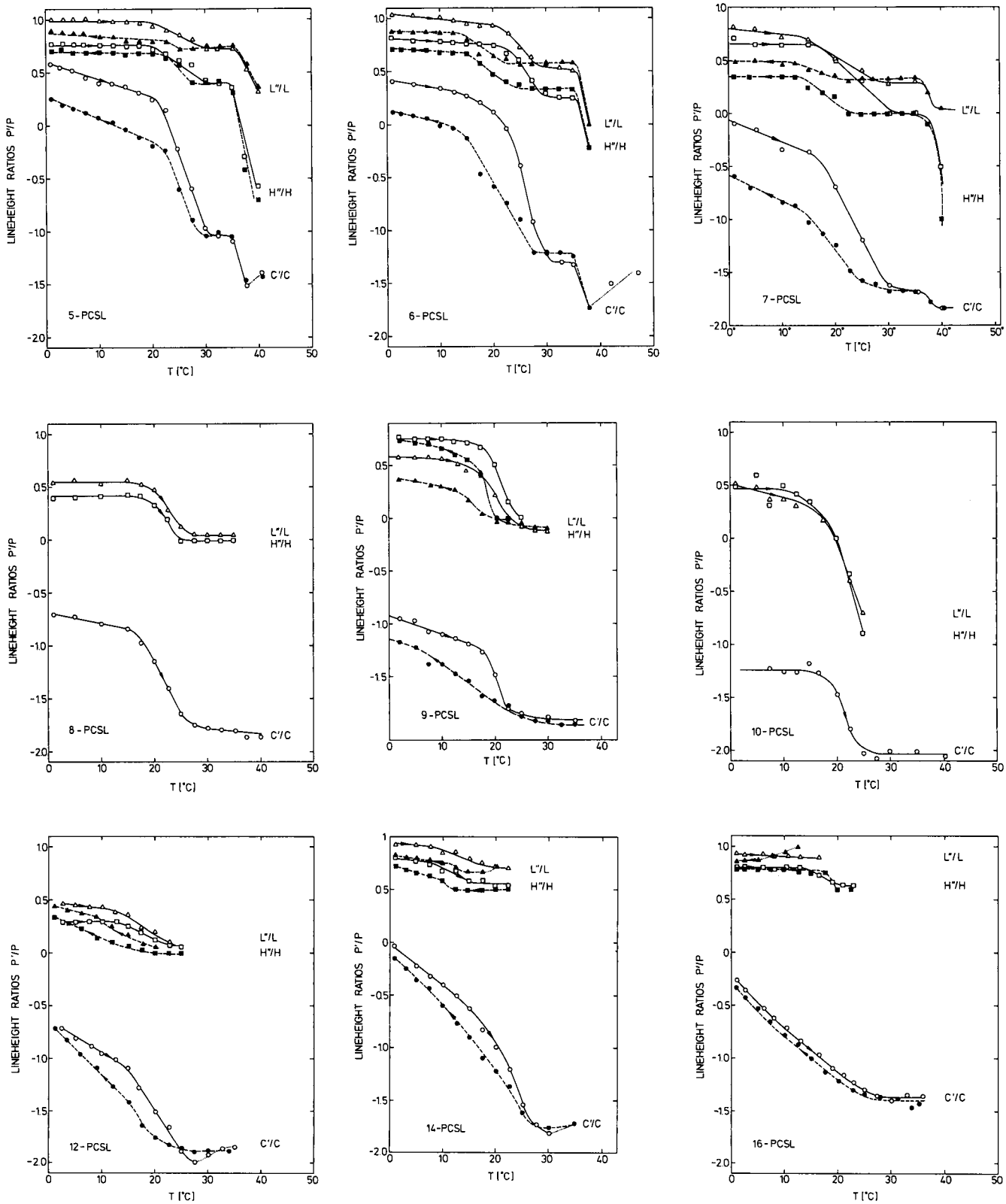


FIGURE 7 Temperature dependence of the diagnostic line height ratios in the second harmonic out-of-phase STESR spectra ($V_2'$ display) of *n*-PCSL phosphatidylcholine spin label positional isomers in gel phase DPPC bilayers. (△) low-field line height ratio, $L''/L$; (○) central line height ratio, $C'/C$; (□) high-field line height ratio, $H''/H$. Open symbols are heating scans and closed symbols are subsequent cooling scans.

recording the height of the central $C'$ line height of the STESR spectrum as the temperature was scanned slowly. This method of recording registers changes in the overall out-of-phase intensity ($V'_2/V_2$), as well as in the $C'/C$ diagnostic line height ratio. Such continuous temperature scans for the different spin label positional isomers are given in Fig. 8. In addition to the pretransitional changes evident at ~25–30°C in the temperature dependence of the line height ratios in Fig. 7, the continuous temperature scans of the $C'$ line height for 5-, 14- and 16-PCSL reveal thermotropic changes taking place at lower temperature. These changes at ~15°C occur only in the first upward temperature scan, not in subsequent upward (or downward) scans, and correspond to the subtransition of DPPC samples that have been incubated at low temperature. The increase in $C'$ observed for 5-PCSL corresponds to alleviation of the spin label segregation on leaving the subgel phase, and the decrease observed with 14- and 16-PCSL corresponds to a true motional effect.

## DISCUSSION

The experiments described above on phosphatidylcholines spin labeled at different positions in the *sn*-2 chain incorporated in gel phase DPPC bilayers indicate two important aspects of STESR studies on systems of high packing density that undergo slow molecular motions. The first is the effect of the saturation behavior on the STESR spectra. In this case, the predominant factor is the spin–spin interaction that occurs for those labels which possess the tendency to phase separate in the closely packed DPPC gel phase. The second aspect concerns the motional characteristics of the lipid chains in gel phase bilayers and the effects of incubation at low temperatures leading to formation of the more stable sub-gel phase.

### Spin–spin interactions and saturation properties

Certain of the *n*-PCSL spin label positional isomers, namely those with the spin label located in the center of the chain, do not mix well with DPPC in the gel phase. This demixing is more pronounced on incubating the samples at low temperature for prolonged periods which leads to conversion of the metastable gel phase to the more stable sub-gel phase. The consequence of this partial segregation of the spin label is an increase in spin–spin interactions that is evident from the spin–spin broadening in the conventional spectrum for incubated samples. Even for nonincubated samples, the spin–spin interactions have a profound effect on the saturation behavior and correspondingly on the saturation transfer spectra, which is in line with the greater sensitivity of $T_1^{eff}$ than of $T_2^{eff}$ to spin–spin interactions. The effect on the STESR spectra arises from the decreased level of saturation evident in the CW saturation studies and which is consequent at least in part on the decrease in effective $T_1$ observed in the saturation recovery experiments.

The result of the spin–spin broadening and decrease in saturation is that the diagnostic STESR line height ratios artefactually reflect an apparently higher degree of rotational mobility when compared with spin labels exhibiting a higher degree of saturation at the same microwave field intensity. Although intrinsic differences in chain mobility in the segregated regions undoubtedly play a role, the observed effects are in agreement with the predictions of the dependence of STESR spectra on $T_1$ obtained by spectral simulation (Thomas and McConnell, 1974; Thomas et al., 1976) and with the experimental dependence on spin label concentration given in Table 2. These findings emphasize the fact that consistent comparisons between the molecular dynamics can be obtained only if the STESR experiments are performed at microwave powers yielding the same degree of saturation, rather than at identical values of the $H_1$ microwave field at the sample. This can most conveniently be achieved by performing CW saturation experiments before the STESR studies. Such considerations are generally valid for systems with different values of $T_1^{eff}$ and do not apply solely to situations involving spin–spin interactions.

### Gel phase chain dynamics

The results from the temperature dependence of the diagnostic STESR line height ratios of the different positional isomers of the *n*-PCSL spin label yield important information on the states of lipid chain mobility in the various low temperature lipid phases. Previous STESR studies using the 5-PCSL spin label in DPPC and DMPC gel phases (Marsh, 1980) have indicated an increase in the rate of rotation about the chain long axis at the pretransition. Such a change was not observed in the gel phase of phosphatidylethanolamines (see also Marsh and Watts, 1980) that do not display a pretransition, but was also observed for phosphatidylglycerols which do possess a pretransition in the negatively charged state (Watts and Marsh, 1981). These conclusions were based on the selective response in the central region ($C'/C$) of the STESR spectrum, as was subsequently further validated by an analysis of the sensitivity of the different regions of the STESR spectrum to

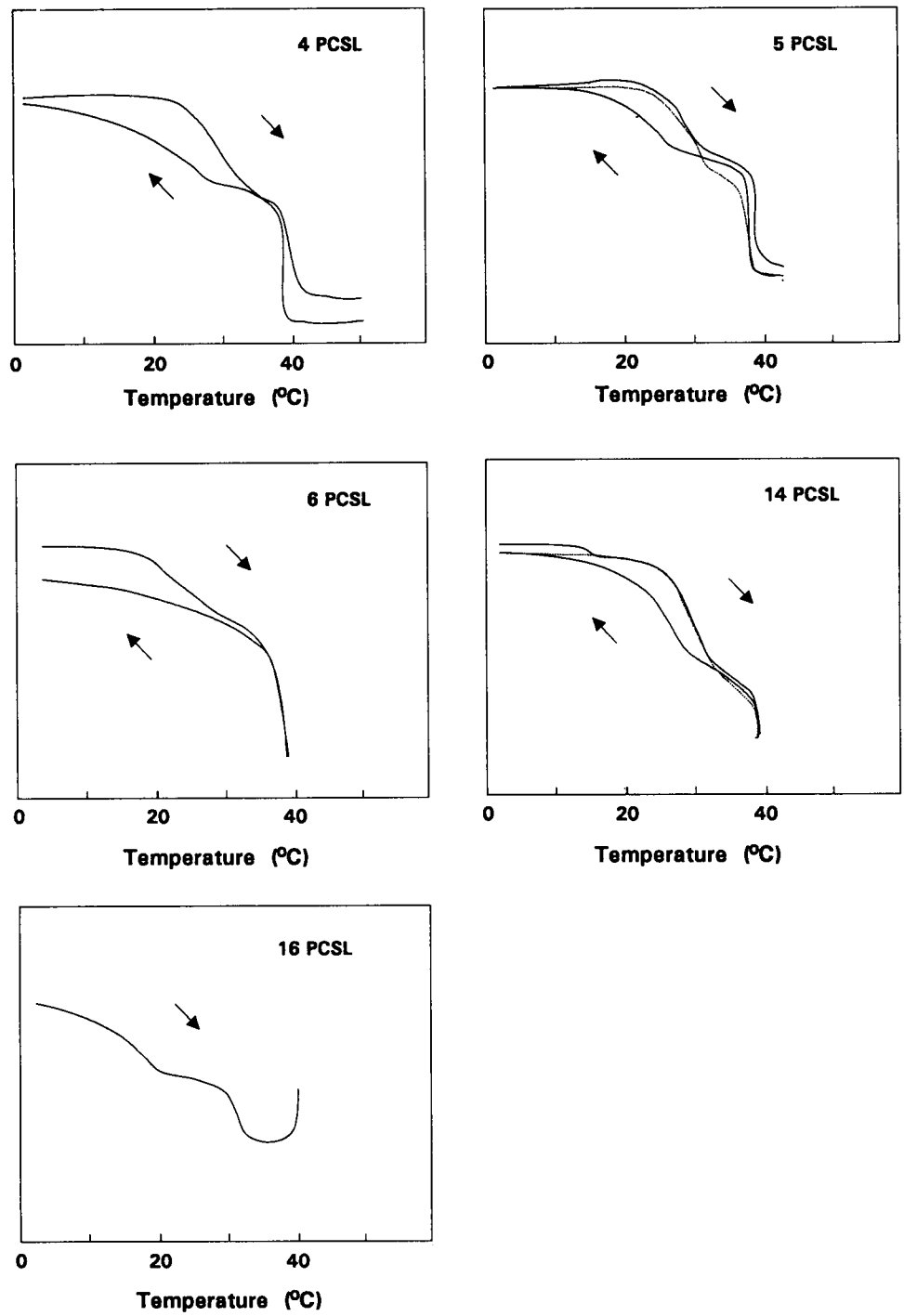


FIGURE 8 Continuous temperature scans of the central line height, $C'$, in the second harmonic out-of-phase STESR spectra ($V_2'$ display) of $n$-PCSL phosphatidylcholine spin label positional isomers in gel phase DPPC bilayers. First heating scan is indicated by the full line and the second heating scan (following the first cooling scan) is indicated by the dashed line. Samples were incubated at 0°C for 60 h, before the first heating scan.

anisotropic rotational diffusion (Fajer and Marsh, 1983; Robinson and Dalton, 1980, and cf also, Gaffney, 1979).

The STESR results that are reported here with the 4-PCSL label in DPPC (Fig. 7) and in dimyristoyl phosphatidylethanolamine (data not shown) are in accord with the previous STESR investigations with the 5-PCSL label in these phospholipid gel phases. However, the results obtained in DPPC with spin label positional isomers located further down the chain indicate that not only does the rate of chain long axis rotation increase at the pretransition, but also there appears to be an increase in segmental mobility of the chain. This is seen from the change that takes place also in the $L''/L$ and $H''/H$ ratios at ~25°C (Fig. 7). Supporting evidence can be found also in Table 3 which lists the effective rotational correlation times deduced from calibrations with isotropically rotating spin labeled hemoglobin. This change in $H''/H$, $L''/L$ and the corresponding effective rotational correlation times is most pronounced for those labels that are located towards the center of the chain and exhibit spin–spin broadening. A possible additional reason for this difference in response is that the orientation of the spin label in the clustered regions of these particular labels may be distorted from that of a normal all-*trans* chain hence giving rise to sensitivity to long axis rotation in the low-field and high-field regions of the spectrum also. The possibility that the chain dynamics may be altered in the clustered regions also must not be excluded.

TABLE 3 **Effective rotational correlation times (μs) deduced from $V_2'$ STESR spectra of different *n*-PCSL spin labels as a function of temperature in gel phase DPPC bilayers***

| *n*-PCSL | | 1°C | 17–20°C | 25–30°C | 34–36°C | 38°C |
|---|---|---|---|---|---|---|
| 4- | $\tau(+1)$ | 55 | 50 | 36 | 34 | 4 |
| | $\tau(-1)$ | 44 | 42 | 28 | 28 | — |
| | $\tau(0)$ | 13 | 5 | 0.5 | 0.3 | 0.03 |
| 5- | $\tau(+1)$ | 88 | 84 | 34 | 21 | 5 |
| | $\tau(-1)$ | 70 | 70 | 20 | 12 | — |
| | $\tau(0)$ | >100 | 13 | 0.3 | 0.3 | 0.07 |
| 6- | $\tau(+1)$ | 88 | 88 | 14 | 9 | — |
| | $\tau(-1)$ | 76 | 76 | 11 | 9 | — |
| | $\tau(0)$ | >100 | 14 | 0.1 | 0.1 | 0.03 |
| 7- | $\tau(+1)$ | 39 | 21 | 3 | 4 | — |
| | $\tau(-1)$ | 46 | 46 | — | — | — |
| | $\tau(0)$ | 5 | 2 | 0.2 | 0.2 | 0.01 |
| 8- | $\tau(+1)$ | 10 | 10 | <1 | <1 | — |
| | $\tau(-1)$ | 24 | — | — | — | — |
| | $\tau(0)$ | 0.8 | 0.5 | 0.02 | 0.02 | 0.01 |
| 9- | $\tau(+1)$ | 12 | 10 | <1 | <1 | — |
| | $\tau(-1)$ | 16 | 18 | <1 | — | — |
| | $\tau(0)$ | 0.4 | 0.15 | 0.02 | 0.02 | — |
| 10- | $\tau(+1)$ | 8 | 4 | <1 | — | — |
| | $\tau(-1)$ | 22 | 16 | <1 | — | — |
| | $\tau(0)$ | 0.15 | 0.13 | 0.02 | 0.01 | — |
| 12- | $\tau(+1)$ | 7 | 4 | <1 | — | — |
| | $\tau(-1)$ | 12 | 11 | <1 | — | — |
| | $\tau(0)$ | 0.7 | 0.2 | 0.01 | 0.01 | — |
| 14- | $\tau(+1)$ | 63 | 55 | 31 | 21 | — |
| | $\tau(-1)$ | 98 | 70 | 34 | 30 | — |
| | $\tau(0)$ | 8 | 3 | 0.9 | 0.15 | — |
| 16- | $\tau(+1)$ | 63 | 55 | — | — | — |
| | $\tau(-1)$ | 86 | 86 | 46 | 40 | — |
| | $\tau(0)$ | 3 | 0.24 | 0.12 | 0.1 | — |

*Effective correlation times $\tau(+1)$, $\tau(-1)$, $\tau(0)$ are those deduced from the $L''/L$, $H''/H$ and $C'/C$ line height ratios, respectively. The temperatures correspond to the limits of the distinct linear regions in Fig. 7, and hence, vary somewhat with label position, the total range of variation being given in each column heading.

Evidence for segmental motion comes not only from the changes at the pretransition, but also from the dependence of the diagnostic STESR line height ratios on spin label isomer position at temperatures below the pretransition (Fig. 5). Such results are essentially in accord with the findings from $^2H$ NMR spectroscopy in which analysis of the reduction in quadrupole splittings and line shapes from $^2H$-labeled chains have demonstrated a limited degree of chain rotational disorder in addition to slow axial diffusion for both phosphatidylcholines and phosphatidylethanolamines in the gel phase (Davis, 1979; Blume et al., 1982; Marsh et al., 1983). Evidence for a limited chain rotational isomerism in the gel phase has also been presented from a detailed analysis of the chain dynamics in conventional spin label ESR spectra (Moser et al., 1989). In addition, it is likely that contributions to the segmental motion arise also from coupled torsional oscillations in the chains, as has been suggested previously (Blume et al., 1982).

Prolonged incubation gives rise to a substantial reduction in the rates of lipid chain motion for the subgel phase relative to the normal gel phase (Fig. 6). The rate of relaxation found for the chain dynamics is considerably longer than that observed for changes in the x-ray diffraction pattern from which it was concluded that the lipid rearrangement is complete in 2 h and the change in hydration within 12 h (Ruocco et al., 1982). The timescale of relaxation in the chain dynamics is more comparable to that required to attain the full calorimetric enthalpy for the subtransition (Chen et al., 1980). Precise statements regarding the extent of chain immobilization in the subgel phase are hampered by the tendency of the spin label to phase separate from the host DPPC lipid. However, continuous temperature scanning STESR spectroscopy provides a useful method for registering the change in chain dynamics at the subtransition (Fig. 8). Particularly interesting is the large response detected with 16-PCSL at the terminal methyl end of the chain. In this connection it is relevant to note that even in the phospholipid crystal structure some rotational twisting is observed towards the terminal methyl ends of the chains (Pearson and Pascher, 1979).

## APPENDIX

# Saturation of powder line shapes for homogeneously and inhomogeneously broadened ESR lines

It is assumed, following Portis (1953), that the individual spin packets saturate independently in a homogeneous manner with the ESR absorption being given by:

$$a(\omega - \omega', H_1) = a_o \cdot g(\omega - \omega')/[1 + \pi\gamma^2 H_1^2 g(\omega - \omega')T_1], \quad \text{(A1)}$$

where $g(\omega - \omega')$ is the line shape function for an individual spin packet centered about $\omega'$. For inhomogeneously broadened lines, the spin packets are distributed according to an envelope function $h(\omega' - \omega_o)$ centered about $\omega_o$. The absorption ESR line shape for a randomly oriented sample is then given by:

$$A_{inh}(\omega, H_1) = \int_{\omega_\perp}^{\omega_\parallel} \int_0^\infty a(\omega - \omega', H_1) \cdot h(\omega' - \omega_o) \cdot I(\omega_o) \cdot d\omega' \cdot d\omega_o, \quad \text{(A2)}$$

where $I(\omega_o)$ is the distribution of inhomogeneously broadened lines corresponding to the different orientations with respect to the static magnetic field direction. This distribution ranges from $\omega_o = \omega_\perp$ to $\omega_o = \omega_\parallel$ which are the resonance positions corresponding to the magnetic field oriented perpendicular and parallel, respectively, to the principal magnetic axis of the spin system.

If it is assumed, also following Portis (1953), that the spin packets are very narrow compared with the inhomogeneous broadening, $g(\omega - \omega')$ will be appreciably different from zero only for $\omega \approx \omega'$. Because $h(\omega' - \omega_o)$ then varies only slowly in this region, it can be replaced by $h(\omega - \omega_o)$ and the two integrals in Eq. A2 may be separated. Doing this, the first derivative ESR display is then given by:

$$dA_{inh}(\omega, H_1)/d\omega = \int_0^\infty a(\omega - \omega', H_1) \cdot d\omega' \cdot \int_{\omega_\perp}^{\omega_\parallel} I(\omega_o) \cdot dh(\omega - \omega_o)/d\omega \cdot d\omega_o + \int_0^\infty da(\omega - \omega', H_1)/d\omega \cdot d\omega' \cdot \int_{\omega_\perp}^{\omega_\parallel} I(\omega_o) \cdot h(\omega - \omega_o) \cdot d\omega_o. \quad \text{(A3)}$$

Changing variable from $\omega'$ and $\omega$ to $\omega - \omega'$ in the first integral of both terms on the right-hand side of Eq. A3 shows that the second term is zero and the first integral in the first term is simply the integrated intensity of a (saturated) spin packet $a(\omega - \omega', H_1)$.

Because the powder line shape distribution $I(\omega_o)$ varies only slowly in the region of $\omega_o = \omega_\parallel$, it may be assumed to be constant in determining the overall line shape in this region of the spectrum (Weil and Hecht, 1963). Changing variables from $\omega$ and $\omega_o$ to $\omega - \omega_o$ in the first term on the right-hand side in Eq. A3, then yields the following expression for the first derivative line shape of the powder pattern in the region of the $\omega_\parallel$ extremum:

$$dA_{inh}(\omega, H_1)/d\omega|_{\omega_\parallel} = I(\omega_\parallel) \cdot h(\omega - \omega_\parallel) \cdot \int_0^\infty a(\omega - \omega', H_1) \cdot d(\omega - \omega'). \quad \text{(A4)}$$

Therefore, the first-derivative powder pattern at the parallel turning point has the inhomogeneous absorption line shape, and saturates in the same way as does the integrated intensity of a single spin packet. Inspection of Eq. (A3) indicates that, as expected, the latter result holds for the entire line shape, provided that the inhomogeneous broadening is sufficiently large that saturation broadening has no effect on the overall powder envelope (cf footnote 2). If it is further assumed that the individual spin packets have a Lorentzian line shape, i.e., $g(\omega - \omega') = (T_2/\pi)/[1 + (\omega - \omega')^2 T_2^2]$, then the integral in Eq. A4 is given by: $a_o/[1 + \gamma^2 H_1^2 T_1 T_2]^{1/2}$. This then corresponds to the saturation behavior described by Eq. 1 above with the value of the exponent being $p = \frac{1}{2}$.

In the absence of inhomogeneous broadening, the powder line shape is given by Eq. A2 with $h(\omega' - \omega_o) = \delta(\omega' - \omega_o)$. The powder line shape at the $\omega_\parallel$ extremum with only homogeneous broadening is then given by the following version of Eq. A4:

$$dA_{hom}(\omega, H_1)/d\omega|_{\omega_\parallel} = I(\omega_\parallel) \cdot a(\omega - \omega_\parallel, H_1). \quad \text{(A5)}$$

Hence, at the parallel turning point, the homogeneously broadened first-derivative powder pattern has the (saturated) homogeneous spin packet absorption line shape and also saturates in the same way as does the spin packet absorption, in essential agreement with the results of Weil and Hecht (1963) and Hubbell and McConnell (1971). For Lorentzian line shapes, this therefore corresponds to a homogeneous saturation behavior which is described by Eq. 1 above with $p = 1$ (cf footnote 2).

Saturation recovery experiments were performed at the National Biomedical ESR Center, Milwaukee, Wisconsin, supported by the National Institutes of Health under grant RR01-008. We wish to thank Prof. J. S. Hyde for extending these facilities to us. Partial support was provided by Florida State University (Piotr Fajer) and by the European Economic Community CODEST program, contract ST2J-0368-C (EDB), (Derek Marsh and Anthony Watts).

*Received for publication 26 July 1991 and in final form 9 October 1991.*

## REFERENCES

Blume, A., D. M. Rice, R. J. Wittebort, and R. G. Griffin. 1982. Molecular dynamics and conformation in the gel and liquid-crystalline phases of phosphatidylethanolamine bilayers. *Biochemistry.* 21:6220–6230.

Chen, S. C., J. M. Sturtevant, and B. J. Gaffney. 1980. Scanning calorimetric evidence for a third phase transition in phosphatidylcholine bilayers. *Proc. Natl. Acad. Sci. USA.* 77:5060–5063.

Clegg, R. M., and W. L. C. Vaz. 1985. Translational diffusion of proteins and lipids in artificial lipid bilayer membranes. A comparison of experiment with theory. *In* Progress in Protein-Lipid Interactions. Vol. 1. A. Watts, and J. J. H. H. M. De Pont, editors. Elsevier, Amsterdam. 173–229.

Davis, J. H. 1979. Deuterium magnetic resonance study of the gel and liquid crystalline phases of dipalmitoyl phosphatidylcholine. *Biophys. J.* 27:339–358.

Eastman, M. P., R. G. Kooser, M. R. Das, and J. H. Freed. 1969. Studies of Heisenberg Spin Exchange in ESR Spectra. I. Linewidth and Saturation Effects. *J. Chem. Phys.* 51:2690–2709.

Fajer, P., and D. Marsh. 1982. Microwave and modulation field inhomogeneities and the effect of cavity Q in saturation transfer

ESR spectra. Dependence on sample size. *J. Magn. Reson.* 49:212–224.

Fajer, P., and D. Marsh. 1983. Sensitivity of saturation transfer ESR spectra to anisotropic rotation. Application to membrane systems. *J. Magn. Reson.* 51:446–459.

Fajer, P., D. D. Thomas, J. B. Feix, and J. S. Hyde. 1986. Measurement of rotational molecular motion by time-resolved saturation transfer electron paramagnetic resonance. *Biophys. J.* 50:1195–1202.

Füldner, H. H. 1981. Characterization of a third phase transition in multilamellar dipalmitoyllecithin liposomes. *Biochemistry.* 20:5707–5710.

Gaffney, B. J. 1979. Spin label-thiourea adducts. A model for saturation transfer EPR studies of slow anisotropic rotation. *J. Phys. Chem.* 83:3345–3349.

Hemminga, M. A., P. A. de Jager, D. Marsh, and P. Fajer. 1984. Standard conditions for the measurement of saturation-transfer ESR spectra. *J. Magn. Reson.* 59:160–163.

Horváth, L. I., and D. Marsh. 1983. Analysis of multicomponent saturation transfer ESR spectra using the integral method: application to membrane systems. *J. Magn. Reson.* 54:363–373.

Horváth, L. I., L. Dux, H. O. Hankovsky, K. Hideg, and D. Marsh. 1990. Saturation transfer electron spin resonance of $Ca^{2+}$-ATPase covalently spin-labeled with β-substituted vinyl ketone- and maleimide-nitroxide derivatives. Effects of segmental motion and labeling levels. *Biophys. J.* 58:231–241.

Hubbell, W. L., and H. M. McConnell. 1971. Molecular motion in spin-labelled phospholipids and membranes. *J. Am. Chem. Soc.* 93:314–326.

Huisjen, M., and J. S. Hyde. 1974. A pulsed EPR spectrometer. *Rev. Sci. Instrum.* 45:669–675.

Kusumi, A., W. K. Subczynski, and J. S. Hyde. 1982. Oxygen transport parameter in membranes as deduced by saturation recovery measurements of spin-lattice relaxation times of spin labels. *Proc. Natl. Acad. Sci. USA.* 79:1854–1858.

Marsh, D. 1980. Molecular motion in phospholipid bilayers in the gel phase: long axis rotation. *Biochemistry.* 19:1632–1637.

Marsh, D. 1982. Electron spin resonance: spin label probes. *Tech. Life Sci.: Biochem.* B4/II, B426/1-B426/44.

Marsh, D., and L. I. Horváth. 1992. Influence of Heisenberg spin exchange on conventional and phase quadrature EPR lineshapes and intensities under saturation. *J. Magn. Reson.* In press.

Marsh, D., and A. Watts. 1980. Molecular motion in phospholipid bilayers in the gel phase: spin label saturation transfer ESR studies. *Biochem. Biophys. Res. Commun.* 94:130–137.

Marsh, D., and A. Watts. 1981. ESR spin label studies of liposomes. *In* Liposomes: From Physical Structure to Therapeutic Applications. C. G. Knight, editor. Elsevier-North Holland, Amsterdam. 139–188.

Marsh, D., and A. Watts. 1982. Spin labeling and lipid-protein interactions in membranes. *In* Lipid-Protein Interactions. Vol. 2. P. C. Jost, and O. H. Griffith, editors. Wiley-Interscience, New York. 53–125.

Marsh, D., A. Watts, and I. C. P. Smith. 1983. Dynamic structure and phase behavior of dimyristoylphosphatidylethanolamine bilayers studied by deuterium magnetic resonance. *Biochemistry.* 22:3023–3026.

Molin, Y. N., K. M. Salikov, and K. I. Zamaraev. 1980. Spin Exchange. Principles and Applications in Chemistry and Biology. Springer-Verlag, Berlin.

Moser, M., D. Marsh, P. Meier, K.-H. Wassmer, and G. Kothe. 1989. Chain configuration and flexibility gradient in phospholipid membranes. Comparison between spin label electron spin resonance and deuterium magnetic resonance, and identification of new conformations. *Biophys. J.* 55:111–123.

Pearson, R. H. and I. Pascher. 1979. The molecular structure of lecithin dihydrate. *Nature (Lond.).* 281:499–501.

Popp, C. A., and J. S. Hyde. 1982. Electron–electron double resonance and saturation recovery studies of nitroxide electron and nuclear spin-lattice relaxation times and Heisenberg exchange rates: lateral diffusion in dimyristoylphosphatidylcholine. *Proc. Natl. Acad. Sci. USA.* 79:2559–2563.

Portis, A. M. 1953. Electronic structure of F centres: Saturation of the electron spin resonance. *Phys. Rev.* 91:1071–1078.

Robinson, B., and L. R. Dalton. 1980. Anisotropic rotational diffusion studied by passage saturation transfer electron paramagnetic resonance. *J. Chem. Phys.* 72:1312–1324.

Ruocco, M. J., and G. G. Shipley. 1982. Characterization of the subtransition of hydrated dipalmitoylphosphatidylcholine bilayers: Kinetic, hydration and structural study. *Biochim. Biophys. Acta.* 691:309–320.

Sachse, J.-H., M. D. King, and D. Marsh. 1987. ESR determination of lipid translational diffusion coefficients at low spin-label concentrations in biological membranes, using exchange broadening, exchange narrowing and dipole–dipole interactions. *J. Magn. Reson.* 71:385–404.

Thomas, D. D., and H. M. McConnell. 1974. Calculation of paramagnetic resonance spectra sensitive to very slow rotational motion. *Chem. Phys. Lett.* 25:470–475.

Thomas, D. D., L. R. Dalton, and J. S. Hyde. 1976. Rotational diffusion studied by passage saturation transfer electron paramagnetic resonance. *J. Chem. Phys.* 65:3006–3024.

Watts, A., and D. Marsh. 1981. Saturation transfer ESR studies of molecular motion in phosphatidylglycerol bilayers in the gel phase. Effects of pretransitions and pH titration. *Biochim. Biophys. Acta.* 642:231–241.

Weil, J. A., and H. G. Hecht. 1963. On the powder lineshape of EPR spectra. *J. Chem. Phys.* 38:281–282.

Yin, J.-J., M. Pasenkiewicz-Gierula, and J. S. Hyde, 1987. Lateral diffusion of lipids in membranes by pulse saturation recovery electron spin resonance. *Proc. Natl. Acad. Sci. USA.* 84:964–968.